Article

Stacking and Not Solely Topology of T Loops Controls Rigidity and Ammonium Ion Movement within d(GTG) G-Quadruplex

Peter Podbevs#ek, Primoz# S#ket, and Janez Plavec

J. Am. Chem. Soc., **2008**, 130 (43), 14287-14293 • DOI: 10.1021/ja8048282 • Publication Date (Web): 04 October 2008

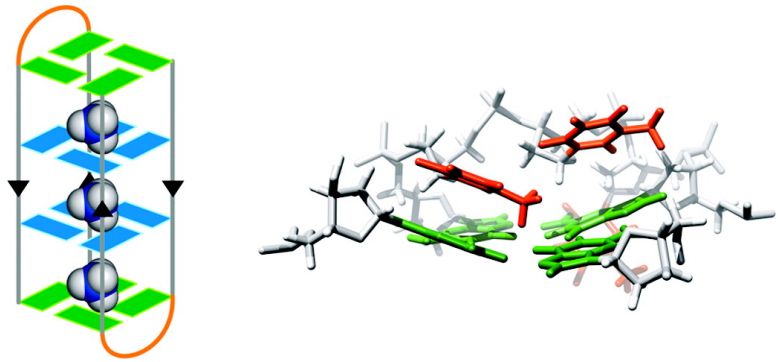

J|A|C|S
ARTICLES

Published on Web 10/04/2008

Stacking and Not Solely Topology of T_3 Loops Controls Rigidity and Ammonium Ion Movement within $d(G_4T_3G_4)_2$ G-Quadruplex

Peter Podbevšek,[†] Primož Šket,[†] and Janez Plavec*[,†,‡]

Slovenian NMR Center, National Institute of Chemistry, Hajdrihova 19, SI-1000 Ljubljana, Slovenia, and Faculty of Chemistry and Chemical Technology, University of Ljubljana, SI-1000 Ljubljana, Slovenia

Received June 24, 2008; E-mail: janez.plavec@ki.si

Abstract: A solution state NMR study has shown that $d(G_4T_3G_4)$ in the presence of $^{15}NH_4^+$ ions folds into a single bimolecular G-quadruplex structure in which its G-tracts are antiparallel and the two T_3 loops span along the edges of the outer G-quartets on the opposite sides of the G-quadruplex core. This head-to-tail topology is in agreement with the topology of the G-quadruplex recently found in the X-ray crystal structure formed by $d(G_4T_3G_4)$ in the presence of K^+ ions [Neidle et al. *J. Am. Chem. Soc.* **2006**, *128*, 5480]. In contrast, the presence of K^+ ions in solution resulted in a complex ensemble of G-quadruplex structures. Molecular models based on NMR data demonstrate that thymine loop residues efficiently base−base stack on the outer G-quartets and in this way stabilize a single structure in the presence of $^{15}NH_4^+$ ions. The use of heteronuclear NMR enabled us to localize three $^{15}NH_4^+$ ion binding sites between pairs of adjacent G-quartets and study the kinetics of their movement. Interestingly, no $^{15}NH_4^+$ ion movement within the G-quadruplex was detected at 25 °C. At 35 °C we were able to observe slow movement of $^{15}NH_4^+$ ions from the outer binding sites to bulk solution with the characteristic residence lifetime of 1.2 s. The slow movement of $^{15}NH_4^+$ ions from the outer binding sites into bulk solution and the absence of movement from the inner binding site were attributed to steric hindrance imposed by the T_3 loops and the rigidity of the G-quadruplex.

Watson−Crick double-stranded DNA is the principal genetic molecule in a cell and is essential for its normal function. Non-B DNA structures of natural repeat sequences have been associated with higher mutation rates and several diseases and disorders.[1−6] G-quadruplex as found in telomeric DNA and other G-rich regions is based on assembly and stacking of G-quartets, a coplanar cyclic arrangement of four guanine nucleotides.[7−11] G-quadruplexes exhibit polymorphism in terms of strand stoichiometry and polarity, orientation across glycosidic bonds, groove dimensions, sequence details, and structure of connecting loops. Structural integrity and stability of G-quadruplexes are invariably connected with the coordination of cations.[12] High-resolution X-ray crystallography[13−18] as well as NMR studies in the solid state[19] and in solution[20−24] have contributed to important progress toward understanding coordination of metal ions within G-quadruplexes. In particular, recent observations by Wu and co-workers showed that alkali metal ions are "NMR

[†] National Institute of Chemistry.
[‡] University of Ljubljana.

(1) Neidle, S.; Balasubramanian, S. *Quadruplex Nucleic Acids*; The Royal Society of Chemistry: Cambridge, 2006; p 301.
(2) Neidle, S.; Read, M. A. *Biopolymers* **2001**, *56*, 195–208.
(3) Rezler, E. M.; Bearss, D. J.; Hurley, L. H. *Curr. Opin. Pharmacol.* **2002**, *2*, 415–423.
(4) Maizels, N. *Nat. Struct. Mol. Biol.* **2006**, *13*, 1055–1059.
(5) Burge, S.; Parkinson, G. N.; Hazel, P.; Todd, A. K.; Neidle, S. *Nucleic Acids Res.* **2006**, *34*, 5402–5415.
(6) De Cian, A.; Lacroix, L.; Douarre, C.; Temime-Smaali, N.; Trentesaux, C.; Riou, J.-F.; Mergny, J.-L. *Biochimie* **2008**, *90*, 131–155.
(7) Gellert, M.; Lipsett, M.; Davies, D. R. *Proc. Natl. Acad. Sci. U.S.A.* **1962**, *48*, 2013–2018.
(8) Keniry, M. A. *Biopolymers* **2001**, *56*, 123–146.
(9) Simonsson, T. *Biol. Chem.* **2001**, *382*, 621–628.
(10) Davis, J. T. *Angew. Chem., Int. Ed.* **2004**, *43*, 668–698.
(11) Phan, A. T.; Kuryavyi, V.; Patel, D. J. *Curr. Opin. Struct. Biol.* **2006**, *16*, 288–298.
(12) Hud, N. V.; Plavec, J. *The Role of Cations in Determining Quadruplex Structure and Stability in Quadruplex Nucleic Acids*; Neidle, S., Balasubramanian, S., Eds.; The Royal Society of Chemistry: Cambridge, 2006; pp 100−130.
(13) Laughlan, G.; Murchie, A. I. H.; Norman, D. G.; Moore, M. H.; Moody, P. C. E.; Lilley, D. M. J.; Luisi, B. *Science* **1994**, *265*, 520–524.
(14) Phillips, K.; Dauter, Z.; Murchie, A. I. H.; Lilley, D. M. J.; Luisi, B. *J. Mol. Biol.* **1997**, *273*, 171–182.
(15) Horvath, M. P.; Schultz, S. C. *J. Mol. Biol.* **2001**, *310*, 367–377.
(16) Haider, S.; Parkinson, G. N.; Neidle, S. *J. Mol. Biol.* **2002**, *320*, 189–200.
(17) Caceres, C.; Wright, G.; Gouyette, C.; Parkinson, G.; Subirana, J. A. *Nucleic Acids Res.* **2004**, *32*, 1097–1102.
(18) Gill, M. L.; Strobel, S. A.; Loria, J. P. *Nucleic Acids Res.* **2006**, *34*, 4506–4514.
(19) Rovnyak, D.; Baldus, M.; Wu, G.; Hud, N. V.; Feigon, J.; Griffin, R. G. *J. Am. Chem. Soc.* **2000**, *122*, 11423–11429.
(20) Schultze, P.; Hud, N. V.; Smith, F. W.; Feigon, J. *Nucleic Acids Res.* **1999**, *27*, 3018–3028.
(21) Deng, H.; Braunlin, W. H. *J. Mol. Biol.* **1996**, *255*, 476–483.
(22) Basu, S.; Szewczak, A.; Cocco, M.; Strobel, S. A. *J. Am. Chem. Soc.* **2000**, *122*, 3240–3241.
(23) Gill, M. L.; Strobel, S. A.; Loria, J. P. *J. Am. Chem. Soc.* **2005**, *127*, 16723–16732.
(24) Ma, L.; Iezzi, M.; Kaucher, M. S.; Lam, Y. F.; Davis, J. T. *J. Am. Chem. Soc.* **2006**, *128*, 15269–15277.

visible" when tightly bound to G-quadruplexes, which offers new insights into cation binding within G-quadruplex channels.[25−32] Correlations between thermodynamic stability, structural details, and cation coordination within G-quadruplexes are far from being understood. The nature of cations is a potential source of great polymorphism with the structural differences of G-quadruplexes formed by the human telomeric sequence in the presence of Na^+ and K^+ ions determined by X-ray crystallography and NMR being a classical example.[33−36] On the other hand, several studies by X-ray crystallography and NMR have shown that $d(G_4T_4G_4)$ folds into the same topology, regardless of the nature of the counterion, which suggests that polymorphism is not universal.

Strand polarities influence the structure of connecting loop residues.[37−42] Nucleobases in edgewise, diagonal, and double-chain reversal loop orientations have been shown to contribute to the stability of G-quadruplex structures through base pairing and stacking over the neighboring G-quartets.[37,42−47] It is noteworthy that loops can adopt diverse structures beyond the basic classification mentioned above, which can be targeted by small molecule ligands.[48,49]

One of the most studied G-quadruplexes, $d(G_4T_4G_4)_2$, is formed by 1.5 units of the telomeric repeat sequence found in the protozoan *Oxytricha nova*. It is well established that it forms a bimolecular G-quadruplex with diagonal T_4 loops in the presence of K^+, Na^+, and $^{15}NH_4^+$ ions.[20] $d(G_4T_3G_4)$, a closely related sequence with one less thymine residue, has been shown by X-ray crystallography to form a head-to-tail bimolecular G-quadruplex in the presence of KCl.[39] Recent solution state NMR studies suggested that the structure formed by $d(G_4T_3G_4)$ in the presence of Na^+ ions is asymmetric or that two G-quadruplexes coexist in solution.[32] The above polymorphic behavior stimulated us to examine G-quadruplex structures formed by $d(G_4T_3G_4)$ in the presence of K^+ and $^{15}NH_4^+$ ions by NMR in solution. A head-to-tail bimolecular G-quadruplex with edgewise T_3 loops on the opposite sides of the G-quadruplex core has been found in the presence of $^{15}NH_4^+$ ions (Figure 1). Folding in the presence of $^{15}NH_4^+$ ions is particularly interesting as they proved to be a very useful probe to determine the number and location of cation binding sites within G-quadruplex structures.[50−55] Furthermore, the kinetics data on $^{15}NH_4^+$ ion movement can give insight into the rigidity of a G-quadruplex.

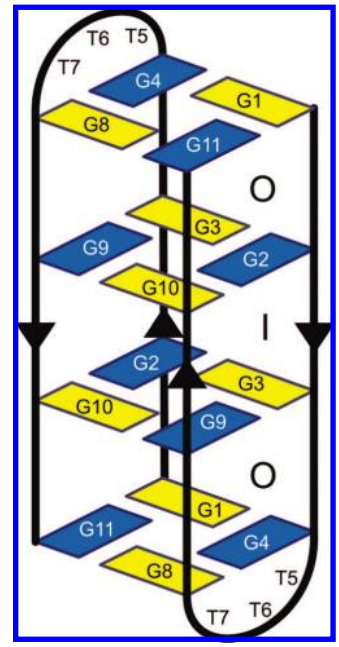

Figure 1. Topology of a bimolecular G-quadruplex $d(G_4T_3G_4)_2$ in the presence of $^{15}NH_4^+$ ions. *Syn* and *anti* guanine bases are shown as yellow and blue rectangles, respectively. Arrows indicate strand orientation. For clarity, thymine bases are not shown. Labels O and I indicate $^{15}NH_4^+$ ion binding sites.

Materials and Methods

Sample Preparation. The oligonucleotide $d(G_4T_3G_4)$ was synthesized on an Expedite 8909 synthesizer using standard phosphoramidite chemistry and removed from the solid support and deprotected with concentrated aqueous ammonia. The last DMT group was retained on the oligonucleotide for purification purposes. DNA was purified using HPLC on a preparative C18 reversed-phase column. Only full-length oligonucleotides were pooled. The DMT group was removed with acetic acid followed by ether extraction. Finally, the small molecular mass impurities were removed by passage through a 1.0 m Sephadex G15 column. Purification steps were followed according to a careful desalting procedure against aqueous LiCl. Samples were lyophilized and

(25) Wu, G.; Wong, A. *Chem. Commun.* **2001**, 2658–2659.
(26) Wong, A.; Fettinger, J. C.; Forman, S. L.; Davis, J. T.; Wu, G. *J. Am. Chem. Soc.* **2002**, *124*, 742–743.
(27) Wu, G.; Wong, A.; Gan, Z. H.; Davis, J. T. *J. Am. Chem. Soc.* **2003**, *125*, 7182–7183.
(28) Wong, A.; Wu, G. *J. Am. Chem. Soc.* **2003**, *125*, 13895–13905.
(29) Wu, G.; Wong, A. *Biochem. Biophys. Res. Commun.* **2004**, *323*, 1139–1144.
(30) Wong, A.; Ida, R.; Wu, G. *Biochem. Biophys. Res. Commun.* **2005**, *337*, 363–366.
(31) Ida, R.; Wu, G. *Chem. Commun.* **2005**, 4294–4296.
(32) Ida, R.; Wu, G. *J. Am. Chem. Soc.* **2008**, *130*, 3590–3602.
(33) Wang, Y.; Patel, D. J. *Structure* **1993**, *1*, 263–282.
(34) Parkinson, G. N.; Lee, P. P. H.; Neidle, S. *Nature* **2002**, *417*, 876–880.
(35) Li, J.; Correia, J. J.; Wang, L.; Trent, J. O.; Chaires, J. B. *Nucleic Acids Res.* **2005**, *33*, 4649–4659.
(36) Luu, K. N.; Phan, A. T.; Kuryavyi, V.; Lacroix, L.; Patel, D. J. *J. Am. Chem. Soc.* **2006**, *128*, 9963–9970.
(37) Risitano, A.; Fox, K. R. *Nucleic Acids Res.* **2004**, *32*, 2598–2606.
(38) Cevec, M.; Plavec, J. *Biochemistry* **2005**, *44*, 15238–15246.
(39) Hazel, P.; Parkinson, G. N.; Neidle, S. *J. Am. Chem. Soc.* **2006**, *128*, 5480–5487.
(40) Hazel, P.; Parkinson, G. N.; Neidle, S. *Nucleic Acids Res.* **2006**, *34*, 2117–2127.
(41) Webba da Silva, M. *Chem.—Eur. J.* **2007**, *13*, 9738–9745.
(42) Rachwal, P. A.; Findlow, I. S.; Werner, J. M.; Brown, T.; Fox, K. R. *Nucleic Acids Res.* **2007**, *35*, 4214–4222.
(43) Keniry, M. A.; Owen, E. A.; Shafer, R. H. *Nucleic Acids Res.* **1997**, *25*, 4389–4392.
(44) Smirnov, I.; Shafer, R. H. *Biochemistry* **2000**, *39*, 1462–1468.
(45) Crnugelj, M.; Hud, N. V.; Plavec, J. *J. Mol. Biol.* **2002**, *320*, 911–924.
(46) Hazel, P.; Huppert, J.; Balasubramanian, S.; Neidle, S. *J. Am. Chem. Soc.* **2004**, *126*, 16405–16415.
(47) Phan, A. T.; Kuryavyi, V.; Ma, J.-B.; Faure, A.; reola, M.-L.; Patel, D. J. *Proc. Natl. Acad. Sci. U.S.A.* **2005**, *102*, 634–639.
(48) Read, M.; Harrison, R. J.; Romagnoli, B.; Tanious, F. A.; Gowan, S. H.; Reszka, A. P.; Wilson, W. D.; Kelland, L. R.; Neidle, S. *Proc. Natl. Acad. Sci. U.S.A.* **2001**, *98*, 4844–4849.
(49) Neidle, S.; Parkinson, G. N. *Biochimie* **2008**, *90*, 1184–1196.
(50) Hud, N. V.; Schultze, P.; Feigon, J. *J. Am. Chem. Soc.* **1998**, *120*, 6403–6404.
(51) Hud, N. V.; Schultze, P.; Sklenar, V.; Feigon, J. *J. Mol. Biol.* **1999**, *285*, 233–243.
(52) Sket, P.; Crnugelj, M.; Plavec, J. *Nucleic Acids Res.* **2005**, *33*, 3691–3697.
(53) Podbevsek, P.; Hud, N. V.; Plavec, J. *Nucleic Acids Res.* **2007**, *35*, 2554–2563.
(54) Sket, P.; Plavec, J. *J. Am. Chem. Soc.* **2007**, *129*, 8794–8800.
(55) Podbevsek, P.; Sket, P.; Plavec, J. *Nucleosides, Nucleotides Nucleic Acids* **2007**, *26*, 1547–1551.

subsequently redissolved in 0.3 mL of 95% H_2O/5% ^2H_2O. LiOH or HCl was added to adjust the pH of NMR samples to 4.5. Oligonucleotide concentration was 2.6 mM per strand.

NMR Spectroscopy. NMR data were collected on Varian VNMRS 600 and 800 MHz NMR spectrometers. All experiments were performed at 25 °C, unless otherwise noted. Standard 1D ^{1}H spectra were acquired with the use of DPFGSE solvent suppression.[56] 2D NOESY spectra were acquired at mixing times of 80 and 250 ms with DPFGSE solvent suppression. Intranucleotide connectivities between imino and aromatic protons were observed in a jump-and-return HMBC spectrum,[57] which was acquired on a natural abundance sample using 2048 transients. The number of $^{15}NH_4^+$ ion binding sites was determined with the use of a ^{15}N−^{1}H HSQC spectrum. $^{15}NH_4^+$ ion movement was followed by a series of ^{15}N−^{1}H NzExHSQC spectra[51,58] at mixing times (τ_m) ranging from 13 ms to 10 s acquired at 25 and 35 °C.

Structure Calculations and Data Analysis. Assignment was performed using Sparky software (UCSF). The structure of loop residues was modeled with the Discover module of the InsightII software (Accelrys). All calculations were performed using the AMBER force field and distance dependent dielectric constant (4r). The coordinates of the crystal structure (pdb ID: 2AVH) were used for the construction of the starting structure. After a 1 ps equilibration stage, simulations continued for 10 ps at temperatures between 300 and 1000 K using a 1.0 fs time step. Only the thymine residues were allowed to move during the NMR restrained molecular dynamics simulation. The resulting structures were subjected to 1000 steps of conjugate gradient minimization. A set of several tents of such calculations converged to the same energy minimum. The resulting structure exhibited very good agreement with NOE derived distance restraints (deviations <0.5Å). Volumes of cross-peaks in ^{15}N−^{1}H NzExHSQC spectra were integrated with Varian VNMRJ 2.1B software. The arbitrary volume of 1.00 in Figure 8 was assigned to the volume of autocorrelation peak I at τ_m of zero. Iterative least-squares fitting was done with Origin 7.5 software (www.originlab.com). Errors in variables are reported as calculated by the Origin program and are estimates of standard deviation.

Results

d($G_4T_3G_4$) Folds into a G-Quadruplex in Solution. ^{1}H NMR spectrum of the aqueous solution of d($G_4T_3G_4$) in the absence of cations showed a broad signal at ca. 11 ppm. During the titration with KCl additional peaks appeared, but even at 50 mM KCl most (80%) of the oligonucleotide was still unfolded. Narrow peaks in the imino region indicated the formation of H-bonds in Hoogsteen geometry, which could be associated with the formation of a G-quadruplex structure (Figure 2). However, the number of resonances suggested formation of several structures. It was impossible to single out an individual G-quadruplex. On the other hand, gradual titration of d($G_4T_3G_4$) with $^{15}NH_4Cl$ gave rise to well resolved ^{1}H NMR spectra, which at a 50 mM concentration of $^{15}NH_4Cl$ pointed to the formation of one major species with only a minute amount (ca. 5%) of other species. Eight resonances could be observed in the imino region of the ^{1}H NMR spectrum which is in agreement with the formation of two (or multiple of two) G-quartets (Figure 2).

d($G_4T_3G_4$) Adopts a Bimolecular G-Quadruplex Structure in the Presence of $^{15}NH_4^+$ Ions. The perusal of the aromatic−anomeric region of NOESY spectra of the oligonucleotide in the presence of $^{15}NH_4^+$ ions revealed four strong H8−H1′ intranucleotide cross-peaks belonging to guanines in the *syn* conformation (G1, G3, G8, and G10). Analysis of NOE connectivities in the aromatic−anomeric (Figure 3A) and aromatic−aromatic (Figure 3B) regions of NOESY spectra showed that each of the guanines in the *syn* conformation has a 3′ neighboring guanine in the *anti* conformation. These 5′-*syn-anti*-3′ dinucleotide steps were substantiated by NOE interactions between H1′ of the 3′ residue with H8 of the 5′ residue which are not observed for standard 5′-*anti-anti*-3′ steps.[59] On the other hand, 5′-*anti-syn*-3′ steps do not give observable sequential NOEs.

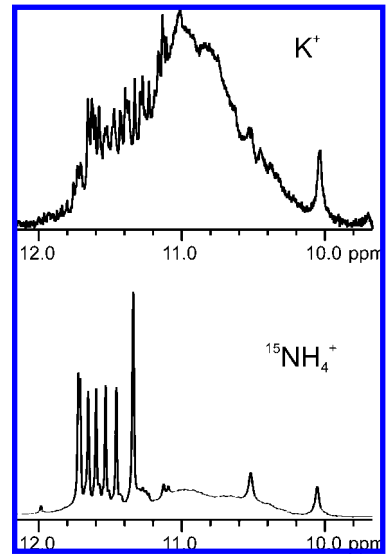

Figure 2. Imino region of ^{1}H NMR spectra of d($G_4T_3G_4$) in the presence of 50 mM concentration of K^+ (top) and $^{15}NH_4^+$ ions (bottom).

Four 5′-*syn-anti-3′* steps between eight guanines along the sequence clearly indicate that the conformation of guanines along the strand is alternating (i.e., 5′-*syn-anti-syn-anti*-T3 loop-*syn-anti-syn-anti*-3′). Spectral assignment was complemented by NOE cross-peaks between imino protons of guanines and protons of the bound $^{15}NH_4^+$ ions (*vide infra*). Moreover, imino protons were correlated with the aromatic protons within the same nucleotide with the use of a jump-and-return HMBC experiment (Figure 3C).[57] Unequivocal correlations of imino and aromatic protons in all guanine residues have enabled complete assignment of all residues in a strand. Furthermore, NH−H8 regions of the NOESY spectra were scrutinized to establish H-bond patterns within individual G-quartets and structural characteristics of the T_3 loops. NOE cross-peaks were consistent with the formation of the following G-quartets: G1→G4→G8→G11 and G10→G9→G3→G2 (arrows indicate sequential NH−H8 cross-peaks around each G-quartet; cross-peaks between the last and first residue of both G-quartets are implied). From H8−H1′ regions of NOESY spectra we have established that the alternation of the glycosidic torsion angles within individual G-quartets is *syn-anti-syn-anti*. In such an arrangement of NH−H8 connectivities, the T3 loop can only adopt an edgewise orientation.

Loop Conformation. The H1′ proton and methyl group of T7 exhibit a strong interstrand cross-peak with the H8 proton of G11 and with imino protons of all four guanines in the outer

(56) Hwang, T. L.; Shaka, A. J. *J. Magn. Reson., Ser. A* **1995**, *112*, 275–279.
(57) Phan, A. T. *J. Biomol. NMR* **2000**, *16*, 175–178.
(58) Montelione, G. T.; Wagner, G. *J. Am. Chem. Soc.* **1989**, *111*, 3096–3098.
(59) Feigon, J.; Koshlap, K. M.; Smith, F. W. *Methods Enzymol.* **1995**, *261*, 225–255.

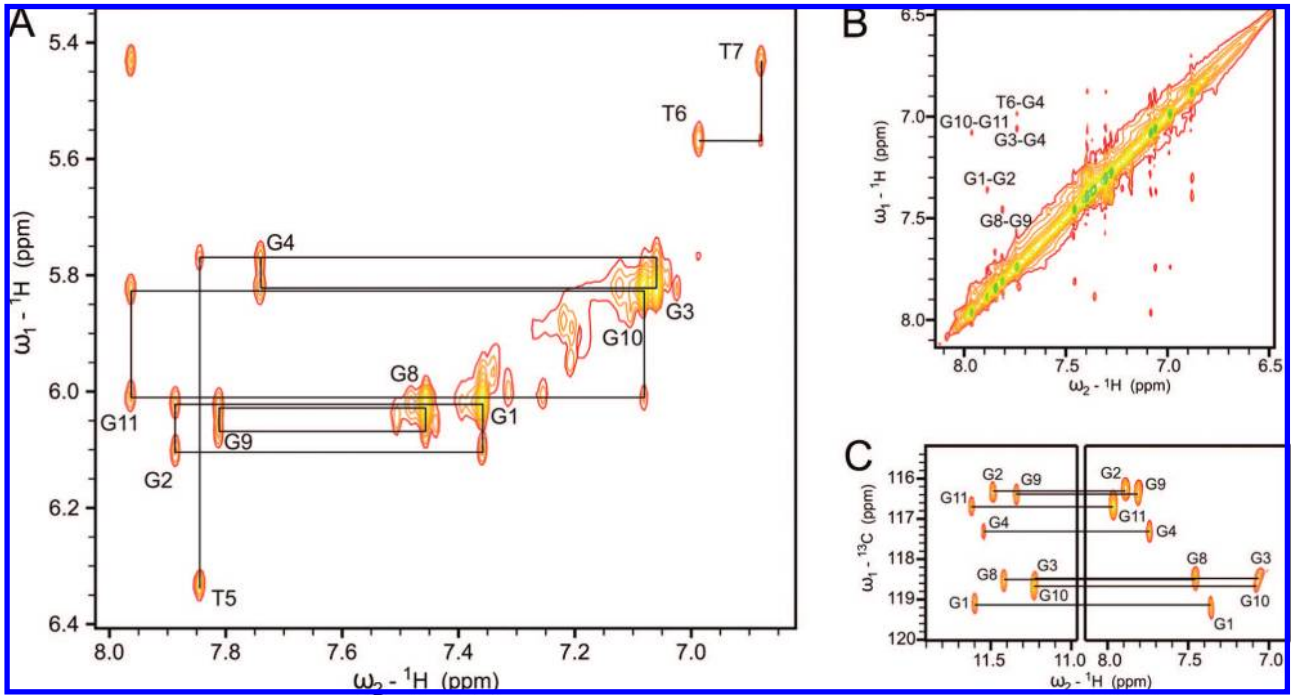

Figure 3. Plots of the aromatic−anomeric (A) and aromatic−aromatic (B) regions of a 250 ms 2D NOESY spectrum of $d(G_4T_3G_4)_2$ at 25 °C in the presence of 50 mM $^{15}NH_4^+$ ions. A jump-and-return HMBC spectrum (C) showing intranucleotide connectivities between imino and aromatic protons.

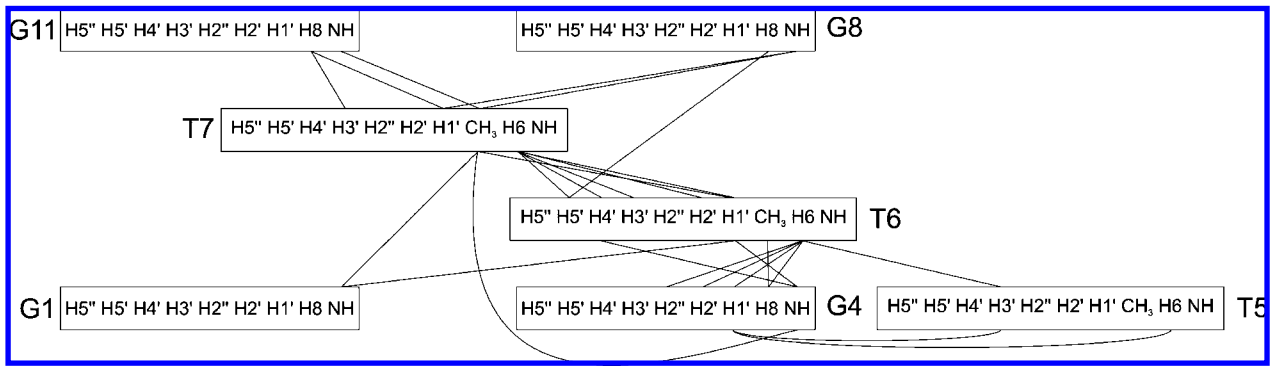

Figure 4. Schematic presentation of internucleotide NOE contacts between loop residues T5−T7 and the outer G-quartet (G1−G4−G8−G11). NH−H8 connectivities inside G-quartet are not shown.

G-quartet, respectively (Figure 4). Aromatic and methyl protons of T6 show connectivities with the H8 proton of G4. T5 shows only sequential connectivities.

On the basis of our NMR data we have constructed a model of the T_3 loops that satisfies NOE restraints. It appears that T6 and T7 are stacked on the outer G-quartets, while T5 is not. The methyl group of T7 is positioned directly over the central cavity of the outer G-quartet. This was substantiated by the presence of the NOE cross-peak between the T7 methyl group and the $^{15}NH_4^+$ ion localized at the outer binding site (*vide infra*). The structure of the T_3 loop obtained by NMR restrained calculations was compared to the X-ray crystal structure (Figure 5). The position of T7 over the outer G-quartet is similar in both structures. On the other hand, T6 is shifted toward the center with a slightly higher distance from the outer G-quartet in the model that fulfills NMR restraints. The orientation of T5 is different in the two structures. In the NMR structure, T5 is positioned in the groove formed by the same oligonucleotide almost in the center between the inner (G3 and G9) and outer (G4 and G8) G-quartets. In the X-ray crystal structure, T5 is oriented toward the same groove but is closer to G4 and

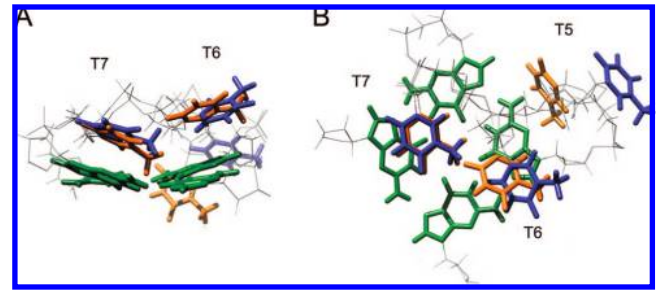

Figure 5. Side (A) and top (B) views of the superposition of the outer G-quartet and T_3 loop from our model and from the X-ray crystal structure (pdb ID: 2AVH)[39] of the $d(G_4T_3G_4)_2$ quadruplex. The guanine bases are shown in green, while the thymine bases of our model and X-ray crystal structure are in orange and blue, respectively.

protrudes away from the G-quadruplex surface. It is noteworthy that NMR derived distances are not consistent with the X-ray crystal structure. The all-atom rmsd value considering the three loop residues in the X-ray crystal structure and our model is

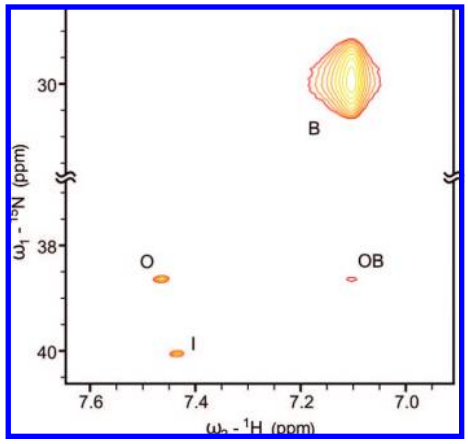

Figure 6. Plot of a 2D $^{15}N-^{1}H$ NzExHSQC spectrum at mixing time of 1.9 s and 35 °C showing autocorrelation peaks for $^{15}NH_4^+$ ions in bulk solution (B), localized at inner (I) and outer (O) binding sites. The cross-peak labeled as OB is attributed to the movement of $^{15}NH_4^+$ ions from the outer binding sites to bulk solution.

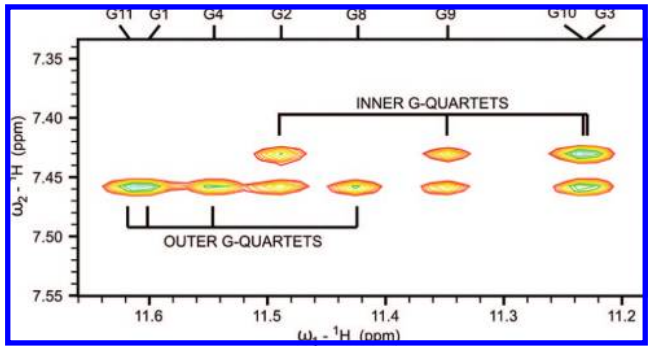

Figure 7. Plot of 2D NOESY spectrum (mixing time of 250 ms) showing connectivities between bound $^{15}NH_4^+$ ions and imino protons of guanines which are a part of either the inner or outer G-quartets.

2.4 Å. The comparison of the structures without taking into account T5 gave an rmsd value of 1.5 Å.

$^{15}NH_4^+$ Ion Localization and Movement. The use of the $^{15}N-^{1}H$ HSQC experiment enables us to observe $^{15}NH_4^+$ ions in different chemical environments (e.g., binding sites). Three $^{15}NH_4^+$ ion binding sites within the $d(G_4T_3G_4)_2$ quadruplex were determined. The most intense autocorrelation peak in the HSQC spectrum with a $\delta(^1H)$ of 7.10 ppm corresponds to $^{15}NH_4^+$ ions in bulk solution. The weaker autocorrelation peak with $\delta(^1H)$ of 7.43 ppm corresponds to bound $^{15}NH_4^+$ ions located at the inner binding site I (cf. Figures 1 and 6). The third autocorrelation peak with a $\delta(^1H)$ of 7.46 ppm corresponds to $^{15}NH_4^+$ ions occupying the two outer binding sites O. The appearance of only a single autocorrelation peak for the two outer binding sites is in agreement with the symmetric nature of the G-quadruplex. It is noteworthy that the ratio of volume integrals of the autocorrelation peaks for the inner and outer binding sites is approximately 1:2.

NOE cross-peaks between imino protons of guanines belonging to either the outer or inner G-quartets and protons of the bound $^{15}NH_4^+$ ions were observed (Figure 7). Imino protons of guanines in the outer G-quartets show NOE connectivities with protons of $^{15}NH_4^+$ ions localized only at the binding site O. On the other hand, imino protons of guanines constituting the inner G-quartets showed NOE connectivities with protons of $^{15}NH_4^+$ ions localized at both O and I binding sites.

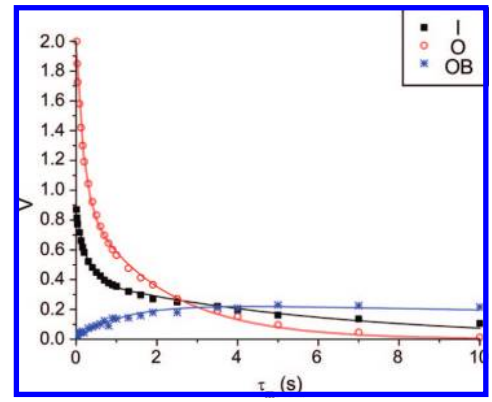

Figure 8. Relative volumes of autocorrelation and cross-peaks as a function of mixing time of $^{15}N-^{1}H$ NzExHSQC experiment.

$^{15}NH_4^+$ ion movement within the G-quadruplex and with bulk solution was followed by acquiring a series of $^{15}N-^{1}H$ NzExHSQC spectra. The NzExHSQC pulse sequence was utilized to detect movement of $^{15}NH_4^+$ ions from their original location to a different chemical environment. The intensity of a cross-peak is directly related to the amount of ions that moved during the user defined mixing time. Rather unexpectedly, we could not observe any exchange cross-peaks in NzExHSQC spectra at 25 °C indicating that the movement of $^{15}NH_4^+$ ions between the binding sites within the $d(G_4T_3G_4)_2$ quadruplex and with bulk solution is very slow or nonexistent. Increasing the sample temperature to 35 °C led to the observation of one weak cross-peak, OB, indicating the movement of $^{15}NH_4^+$ ions from the outer binding sites to bulk solution (Figure 6). No cross-peaks for the movement between the outer and inner binding sites could be observed even at this temperature. Temperature could not be increased further as the G-quadruplex started to undergo melting at the concentration of the NMR sample. For comparison, UV measurements established a melting temperature of 35.6 °C.

Quantitative Assessment of $^{15}NH_4^+$ Ion Movement. Autocorrelation and exchange cross-peaks were further evaluated in a quantitative manner. Volume intensities of autocorrelation peaks O and I are reduced with increasing mixing time due to the movement of ions and relaxation (Figure 8). While the decrease of autocorrelation peak I is faster than that of O at short mixing times, it approaches zero with a much smaller slope at mixing times longer than 2 s. The differences are related to the distinct kinetics of $^{15}NH_4^+$ ion movement from the two binding sites. The volume of autocorrelation peaks can be described by a biexponential function of mixing time.[53,54,60] The OB cross-peak arises due to the movement of $^{15}NH_4^+$ ions from the outer binding site into bulk solution. The predominant increase of the OB cross-peak volume due to movement of ions is counteracted by relaxation which leads to its decrease at longer mixing times (Figure 8). An additional factor that has to be considered in the analysis of the cross-peak volume is efficient proton exchange with solvent as soon as $^{15}NH_4^+$ ions move into bulk solution. This causes considerable loss of volume of the OB cross-peak.[54] The above factors are included in the following equation (eq 1):

$$V_{cross}(\tau_m) = A\ e^{-T_1^{-1}\tau_m}(1 - e^{-k\tau_m}) \quad (1)$$

where V_{cross} is the cross-peak volume, A is the proportionality factor which also accounts for proton exchange with solvent, k is the exchange rate constant, T_1 is the ^{15}N longitudinal

relaxation time, and τ_m is the mixing time. Parameters A and k were freely optimized during the iterative fitting procedure of the volumes of the OB cross-peak to eq 1, while T_1 was fixed to 41 s (calculated through the analysis of autocorrelation peak B). A good fit (rmsd = 0.02) was obtained (Figure 8). The exchange rate constant for the movement of $^{15}NH_4^+$ ions from the outer binding site to the bulk solution at 35 °C is 0.8 ± 0.1 s^{-1}. The corresponding residence lifetime of $^{15}NH_4^+$ ions at the binding site O is 1.2 ± 0.1 s at 35 °C and pH 4.5. The signal loss due to proton exchange with bulk water (parameter A) was 87 ± 1%.

Discussion

The high-resolution structure of the bimolecular G-quadruplex adopted by $d(G_4T_3G_4)$ in the presence of K^+ ions has been determined recently by X-ray crystallography.[39] It is interesting to note that the single substitution in the T_3 loop by a 5′-bromo-uridine in $d(G_4{}^{Br}UTTG_4)$ leads to the formation of a head-to-tail as well as a stacked head-to-head dimeric structure (pdb ID: 2AVJ).[39] The parent sequence $d(G_4T_3G_4)$ forms a head-to-tail G-quadruplex (pdb ID: 2AVH).[39] Recently, Wu and co-workers have noted a large number of imino ^1H NMR signals for the same oligonucleotide in the presence of Na^+ ions indicating an asymmetric bimolecular G-quadruplex or the coexistence of two symmetric bimolecular G-quadruplexes in solution.[32] Our current NMR study has demonstrated that $d(G_4T_3G_4)$ folds into a single bimolecular G-quadruplex in the presence of $^{15}NH_4^+$ ions, while several G-quadruplex structures form in the presence of K^+ ions. After careful analysis of the NMR data we could conclude that the oligonucleotide $d(G_4T_3G_4)$ in the presence of $^{15}NH_4^+$ ions adopts a head-to-tail topology where its G-tracts are antiparallel. Structure consists of four G-quartets and two T_3 loops in an edgewise orientation on the opposite sides of the G-quadruplex core.

Three $^{15}NH_4^+$ ion binding sites were identified within the $d(G_4T_3G_4)_2$ G-quadruplex. They are located between pairs of two adjacent G-quartets. No evidence was found for $^{15}NH_4^+$ ion binding sites between the outer G-quartets and T_3 loops. Previous studies have shown that $^{15}NH_4^+$ ions move both between binding sites within G-quadruplexes and with bulk solution. However, the ionic radius of the $^{15}NH_4^+$ ion is too large to allow it free passage through the central ion cavity of G-quartets. Therefore, $^{15}NH_4^+$ ion movement must be coupled with at least partial opening of the G-quartets suggesting that its movement is in direct relation with the stiffness of the individual G-quartet and the overall G-quadruplex structure. As no $^{15}NH_4^+$ ion movement was detected at temperatures up to 25 °C, the $d(G_4T_3G_4)_2$ quadruplex must be sufficiently rigid to hinder the passage of $^{15}NH_4^+$ ions. The exchange rate constant for the movement from the outer binding sites of the $d(G_4T_3G_4)_2$ quadruplex into bulk solution is 0.8 s^{-1} at 35 °C. Our NMR data suggest that the edgewise T_3 loops in the $d(G_4T_3G_4)_2$ quadruplex contribute to the stiffness of the G4/G8 base pair within the same oligonucleotide making it more difficult for the outer G-quartet to slightly open and allow movement of $^{15}NH_4^+$ ions through the outer G-quartet. In addition, stacking interactions of loop residues with G11 belonging to the other oligonucleotide molecule add to the rigidity and thus contribute to stiffness and restrict the breathing dynamics of the $d(G_4T_3G_4)_2$ quadruplex. Efficient stacking of T6 and T7 over the center of the outer G-quartets places these two residues in a conformation that sterically hinders the passage of $^{15}NH_4^+$ ions through $d(G_4T_3G_4)_2$.

A related oligonucleotide, $d(G_4T_4G_4)$ adopts a bimolecular fold-back topology with T_4 loops spanning across the diagonals of the outer G-quartets.[16,18,23,61−63] $d(G_4T_4G_4)$ differs from the oligonucleotide under study in only an additional thymine in the loop which, however, leads to rather dramatic differences in topologies of respective G-quadruplexes. The longer loops prefer diagonal over edgewise orientation. Perusal of the 3D structure of $d(G_4T_4G_4)_2$ (PDB ID: 156D)[62] shows that individual thymine residues of the loops are positioned around the central ion cavity of the outer G-quartets. In such a structure, loop residues do not represent a steric barrier for $^{15}NH_4^+$ ions to enter or leave the interior of the G-quadruplex. As a result relatively fast movement of $^{15}NH_4^+$ ions through the G-quartets in $d(G_4T_4G_4)_2$ has been observed. We have determined the exchange rate constant (k_{OB}) of 6 s^{-1} at 25 °C for the movement of $^{15}NH_4^+$ ions from the outer binding site of $d(G_4T_4G_4)_2$ to bulk solution (data not published). Even at 35 °C, the corresponding $^{15}NH_4^+$ ion movement from $d(G_4T_3G_4)_2$ is 7-fold slower. The exchange rate constant (k_{IO}) for the movement of $^{15}NH_4^+$ ions from the inner to the outer binding sites of $d(G_4T_4G_4)_2$ is 3.7 s^{-1} at 25 °C.[64] No such movement occurs within $d(G_4T_3G_4)_2$ even at 35 °C.

The $d(G_3T_4G_4)$ oligonucleotide forms a bimolecular parallel/antiparallel (3 + 1) G-quadruplex with three G-quartets, a diagonal, and an edge-type loop.[65] The 3D structure (PDB ID: 1U64) shows that the four thymine residues of the edge-type loop are positioned along the side of the outer G-quartet and do not obstruct the movement of $^{15}NH_4^+$ ions through the outer G-quartet.[52,65,66] As a result the exchange rate constant (k_{UB}) is 7.2 s^{-1} for movement from $d(G_3T_4G_4)_2$ at 25 °C which is 9-fold faster[54] than that from $d(G_4T_3G_4)_2$ at 35 °C. In full agreement, $^{15}NH_4^+$ ion movement across the diagonal loop of $d(G_3T_4G_4)_2$ exhibiting considerable stacking interactions over the outer G-quartet is characterized by an exchange rate constant (k_{LB}) of 0.6 s^{-1} at 25 °C.

The unimolecular G-quadruplex formed by $d[G_4(T_4G_4)_3]$ features two edgewise T_4 loops spanning the edges of the same outer G-quartet together with a diagonal loop on the other side of the G-quadruplex core.[53,67,68] The solution structure in the presence of Na^+ ions has shown that the two edgewise T_4 loops are not well-defined which therefore suggests their higher mobility.[67,68] We have recently determined an exchange rate constant (k_{O2B}) of 0.75 s^{-1} at 20 °C for the movement of $^{15}NH_4^+$ ions through the outer G-quartet of $d[G_4(T_4G_4)_3]$ spanned with the two edgewise T_4 loops.[53] In comparison the exchange rate constant (k_{O1B}) for the movement of $^{15}NH_4^+$ ions through the outer G-quartet spanned by a diagonal T_4 loop was 0.16 s^{-1} at 20 °C. The higher flexibility of the loops is associated with faster movement of $^{15}NH_4^+$ ions through the outer G-quartet.

(60) Quantitative analysis of autocorrelation peaks according to the biexponential funtion reported previously: (binding site I) $f = 0.53 \pm 0.02$, $d_1 = 3.95 \pm 0.33$ s^{-1}, $d_2 = 0.17 \pm 0.01$ s^{-1}; (binding site O) $f = 0.53 \pm 0.02$, $d_1 = 5.58 \pm 0.41$ s^{-1}, $d_2 = 0.49 \pm 0.03$ s^{-1}.

(61) Smith, F. W.; Feigon, J. *Nature* **1992**, *356*, 164–168.
(62) Schultze, P.; Smith, F. W.; Feigon, J. *Structure* **1994**, *2*, 221–233.
(63) Dingley, A. J.; Peterson, R. D.; Grzesiek, S.; Feigon, J. *J. Am. Chem. Soc.* **2005**, *127*, 14466–14472.
(64) Sket, P.; Crnugelj, M.; Kozminski, W.; Plavec, J. *Org. Biomol. Chem.* **2004**, *2*, 1970–1973.
(65) Crnugelj, M.; Sket, P.; Plavec, J. *J. Am. Chem. Soc.* **2003**, *125*, 7866–7871.
(66) Sket, P.; Crnugelj, M.; Plavec, J. *Bioorg. Med. Chem.* **2004**, *12*, 5735–5744.
(67) Wang, Y.; Patel, D. J. *J. Mol. Biol.* **1995**, *251*, 76–94.
(68) Smith, F. W.; Schultze, P.; Feigon, J. *Structure* **1995**, *3*, 997–1008.

Insights into intricate relations of loop size and topology with respect to their role in cation-dependent stabilization of G-quadruplexes are important for understanding their function as well as for the design of ligands that target specific structural features of G-quadruplex forming sequences in the genome. Examination of the kinetics of $^{15}NH_4^+$ ion movement gives important insights into the rigidity of G-quartets in connection with conformational plurality of loops and their pertinence to the overall structural setup of G-quadruplexes.

Conclusions

The oligonucleotide $d(G_4T_3G_4)$ in the presence of K^+ ions forms an ensemble of G-quadruplex structures, while the presence of $^{15}NH_4^+$ ions favor the formation of a single G-quadruplex structure in solution. This structure features four G-quartets with two T_3 loops spanning the edges of the outer G-quartets on opposite sides of the G-quadruplex core. Such head-to-tail topology is in agreement with the bimolecular G-quadruplex found in the X-ray crystal structure of $d(G_4T_3G_4)_2$ in the presence of K^+ ions.[39] Heteronuclear NMR was utilized to establish three $^{15}NH_4^+$ ion binding sites between pairs of adjacent G-quartets. No $^{15}NH_4^+$ ion movement within the G-quadruplex was detected at temperatures up to 25 °C. Only relatively slow movement of $^{15}NH_4^+$ ions from the outer binding sites to bulk solution was observed at 35 °C with an exchange rate constant of 0.8 s^{-1}. The slow movement of $^{15}NH_4^+$ ions was attributed to the structural features of the T_3 loops, which are stacked over the central cavity of the outer G-quartet and represent a steric barrier for the movement of $^{15}NH_4^+$ ions. In addition, stacking of loop thymine residues on the outer G-quartet contributes to the G-quartet's rigidity and adds to an unfavorable barrier for the movement of $^{15}NH_4^+$ ions, which requires partial opening of the G-quartets.

Acknowledgment. We thank Slovenian Research Agency (ARRS) and the Ministry of Higher Education, Science and Technology of the Republic of Slovenia (Grant Nos. P1-0242 and J1-0986) for their financial support.

JA8048282